Published in final edited form as:
Cancer Cell. 2012 March 20; 21(3): 333–347. doi:10.1016/j.ccr.2012.01.010.

Deconstruction of the SS18-SSX Fusion Oncoprotein Complex: Insights into Disease Etiology and Therapeutics

Le Su[1], **Arthur V. Sampaio**[1], **Kevin B. Jones**[2,4], **Marina Pacheco**[3], **Angela Goytain**[3], **Shujun Lin**[1], **Neal Poulin**[3], **Lin Yi**[1], **Fabio M. Rossi**[1], **Juergen Kast**[1], **Mario R. Capecchi**[4], **T. Michael Underhill**[1], and **Torsten O. Nielsen**[3]

[1]Biomedical Research Centre, 2222 Health Sciences Mall, University of British Columbia, Vancouver, BC, Canada, V6T 1Z3

[2]Department of Orthopaedics and Center for Children's Cancer Research, Huntsman Cancer Institute, University of Utah, Salt Lake City, UT 84112, United States

[3]Department of Pathology and Laboratory Medicine, 2222 Health Sciences Mall, University of British Columbia, Vancouver, BC, Canada, V6T 1Z3

[4]Department of Human Genetics and Howard Hughes Medical Institute, University of Utah, Salt Lake City, UT 84112, United States

SUMMARY

Synovial sarcoma is a translocation-associated sarcoma where the underlying chromosomal event generates *SS18-SSX* fusion transcripts. In vitro and in vivo studies have shown that the SS18-SSX fusion oncoprotein is both necessary and sufficient to support tumorigenesis; however, its mechanism of action remains poorly defined. We have purified a core SS18-SSX complex and discovered that SS18-SSX serves as a bridge between activating transcription factor 2 (ATF2) and transducin-like enhancer of split 1 (TLE1), resulting in repression of ATF2 target genes. Disruption of these components by siRNA knockdown or treatment with HDAC inhibitors rescues target gene expression, leading to growth suppression and apoptosis. Together, these studies define a fundamental role for aberrant ATF2 transcriptional dysregulation in the etiology of synovial sarcoma.

INTRODUCTION

Synovial sarcoma is an aggressive soft-tissue tumor of adolescents and young adults (Haldar et al., 2008). Histologically, these tumors can display monophasic (spindle shaped mesenchymal cells), biphasic (similar but with focal epithelial differentiation) or poorly differentiated (small blue round cells generic with some other translocation-associated sarcomas) morphology. Treatment consists of wide local tumor excision and radiation, which cures local disease. Metastatic disease is usually fatal despite treatment with

Address correspondence to: T. Michael Underhill, Biomedical Research Centre, 2222 Health Sciences Mall, University of British Columbia, Vancouver, British Columbia, Canada, V6T 1Z3. Tel: 640.822.5833. Fax: 604.822.7815. tunderhi@brc.ubc.ca.

SUPPLEMENTAL INFORMATION

Supplementary information includes supplementary experimental procedures and seven figures.

conventional chemotherapy agents such as doxorubicin and ifosphamide, which confer at best a temporary response.

Almost all synovial sarcomas carry a demonstrable, pathognomonic t(X;18) reciprocal translocation fusing *SS18* to an *SSX* gene. Clinical diagnosis can be molecularly confirmed by the identification of this event by karyotyping, RT-PCR or FISH techniques, although recently TLE1 has emerged as a useful immunohistochemical marker that may obviate the need to resort to molecular testing (Jagdis et al., 2009). A variety of studies have shown that the resulting SS18-SSX fusion functions as an oncoprotein; heterologous expression induces transformation of rat fibroblasts, and continued expression is needed for tumor cell survival (Nagai et al., 2001). Most convincingly, in transgenic mice conditional overexpression of SS18-SSX2 in the myogenic progenitor compartment, but not other compartments, leads to the appearance of both monophasic and biphasic synovial sarcoma tumors with full penetrance (Haldar et al., 2007). Together, these studies indicate that the SS18-SSX fusion protein exhibits oncogenic activity and is both necessary and sufficient for tumorigenesis.

The SS18-SSX fusion protein retains a C-terminal repressor domain from either of two highly similar cancer-testis antigens, SSX1 or SSX2 (SSX4 has also been reported in rare cases), which is fused to the N-terminus of SS18, a transcriptional coactivator (Ladanyi, 2001). The resulting fusion proteins SS18-SSX1 and SS18-SSX2 have no apparent DNA-binding motif, yet appear to function predominantly in transcriptional regulation (Lim et al., 1998). The control of gene expression by SS18-SSX is believed to involve chromatin remodeling, due to its colocalization with both Trithorax (TrxG) and Polycomb group (PcG) complexes, maintaining chromatin in a poised bivalent state (de Bruijn et al., 2006; Lubieniecka et al., 2008; Soulez et al., 1999). Similar to other sarcoma-associated fusion oncoproteins, expression of SS18-SSX contributes to aberrant transcriptional activity and dysregulated gene expression. Since SS18-SSX itself lacks direct DNA-binding domains or activity, it has been challenging to identify target genes or to decipher its mechanism of action. In this report, we explore the mechanism of SS18-SSX-mediated repression and its connection with the anti-tumor action of HDAC inhibitors by identifying the key constituents of SS18-SSX transcriptional complexes in synovial sarcoma.

RESULTS

To study transcriptional regulation governed by SS18-SSX, we used a validated antibody (RA2009, Figure S1A) to isolate endogenous SS18-SSX2 and its interactants from human synovial sarcoma SYO-1 cells (Figure 1A). Mass spectroscopy further confirmed the presence of SS18-SSX2 (Figure S1B) and identified several known cofactors, including histone deacetylases (Figure S1C). This approach also allowed us to capture multiple peptides corresponding to two previously uncharacterized components, ATF2 and TLE1 (Figure S1C). Both of these are master transcriptional regulators that are highly conserved across different species. ATF2 is a DNA-binding protein that recognizes the cAMP-responsive element (CRE) via its leucine zipper domain and recruits histone acetyltransferases (HATs) to increase transcription (Kawasaki et al., 2000). However, the other component TLE1 is a *Groucho* co-repressor that usually interacts with transcriptional activators and functions in a dominant-negative manner to inhibit transcription (Ali et al., 2010). TLE1 is known to be highly expressed in synovial sarcoma (Terry et al., 2007) and has recently been demonstrated to be a robust diagnostic marker for synovial sarcoma, although its biological function in this disease has been unclear (Foo et al., 2011; Jagdis et al., 2009; Knosel et al., 2010).

To validate the proteomic data, immunoprecipitation (IP) was performed in two human synovial sarcoma cell lines (SYO-1 and FUJI), and this shows that both ATF2 and TLE1 are

specifically precipitated with anti-SS18-SSX, but not with rabbit IgG (Figure 1B and Figure S1D). Interaction of SS18-SSX2 with both ATF2 and TLE1 was preserved in the presence of ethidium bromide (EtBr, Figure 1B), which suggests that this fusion oncoprotein complex forms independently of DNA. ATF2 and TLE1 association with both SS18-SSX1 and SS18-SSX2 fusion proteins was verified by reciprocal IP using RA2009, ATF2, and TLE1 antibodies (Figure 1C) using patient primary tumors confirmed to express *SS18-SSX1* and *SS18-SSX2* (Figure S1E). Importantly, we find that the mouse homologs of ATF2 (mATF2) and TLE1 (mTLE1/Grg1) are also bound to the human fusion protein in cell cultures derived from tumors from *SS18-SSX2* conditional overexpression mice (Figure 1C) (Haldar et al., 2007). The specificity of ATF2-TLE1 association was confirmed by reciprocal IP using a clear cell sarcoma cell line (DTC-1) where, in the absence of the SS18-SSX fusion oncoprotein, ATF2 and TLE1 no longer co-immunoprecipitated (Figure S1F). This raised the possibility that SS18-SSX serves as a scaffold to link ATF2 and TLE1. Indeed, glycerol-gradient fractionation on human synovial sarcoma SYO-1 cells revealed a co-elution profile of ATF2 and TLE1 with SS18-SSX2 (Figure 1D and Figure S1G), indicating that ATF2 and TLE1 occur in the same SS18-SSX complex. We also observed several fundamental chromatin-remodeling factors (SMARCA2, HDAC1 and EZH2) in a major overlapping peak with SS18-SSX2 (Figure S1G).

To obtain further evidence of the observed disease-specific abnormal association of ATF2 with TLE1, a small interfering RNA (siRNA)-based method was used to deplete endogenous SS18-SSX2 and its complex components ATF2 and TLE1 in human SYO-1 and mouse synovial sarcoma cells (Figures S2A and S2B), and the consequences on cell survival was assessed. Similar to SS18-SSX2 knockdown, both ATF2 and TLE1 silencing reduces synovial sarcoma cell growth (Figure 2A and Figure S2C) and impairs the ability of human and mouse tumor cells to form colonies (Figure 2B and Figure S2D). These knockdown cells appear to undergo apoptosis since depletion of either ATF2 or TLE1 induces an enrichment in the Annexin-V^+ fraction (Figure 2C) and also stimulates Caspase-3 activation (Figure S2E). Together, these data demonstrate that ATF2 and TLE1 functionally associate with SS18-SSX to form an endogenous complex in synovial sarcoma important for tumor cell survival.

To gain molecular insights into SS18-SSX complex assembly, reciprocal IP was performed on human SYO-1 cells transfected with non-specific, SS18-SSX2, ATF2, or TLE1 siRNA. Western blot analysis shows that ATF2 and TLE1 co-immunoprecipitation is dependent upon SS18-SSX2 (Figure 3A). By contrast, recruitment of ATF2 and TLE1 to SS18-SSX2 seems to be independent of each other because depletion of ATF2 (or TLE1) has no significant impact on SS18-SSX2 association with TLE1 (or ATF2) (Figure 3B). To further confirm binding specificity, HEK293 cell lines stably expressing Myc-tagged *SS18*, *SS18-SSX2*, or empty vector were generated (Figure S3A). Analysis of the anti-Myc-tag precipitates reveals the co-existence of ATF2 and TLE1 with recombinant SS18-SSX2 (Figure 3C). The lack of TLE1, but not ATF2, in the Myc-SS18 precipitates (Figure 3C) indicates that ATF2 and TLE1 recruitment involves different protein domains of SS18-SSX2. Reciprocal IP of ATF2 and TLE1 also supports this concept by showing that their connection depends on the presence of SS18-SSX2 and does not occur with SS18 alone (Figures S3B and S3C). Consistent with these data, we find that compared to control cells, ATF2 and TLE1 migrate as individual glycerol-gradient peaks in *SS18-SSX2*-knockdown cells (Figure 3D), implying that they are not found in a shared complex in the absence of SS18-SSX. The shared change in ATF2 and TLE1 distribution in glycerol-gradient sedimentation was also observed in HEK293 stable cell lines with and without the fusion oncoprotein (Figure S3D). To address which domains of SS18-SSX are responsible for ATF2 and TLE1 binding, we next generated *SS18-SSX2* deletion mutants (Figure 3E and Figure S3E) (Nagai et al., 2001) and performed reciprocal IP using the antibodies specific to

Myc-tag, ATF2, and TLE1 in HEK293 cells. The results suggest that the N-terminal SNH (SYT N-terminal homolog) domain is responsible for the interaction of SS18-SSX2 with ATF2, whereas TLE1 specifically interacts with the repressor domain (SSXRD) of SS18-SSX2 (Figure 3F). In aggregate, these data further reinforce that S18-SSX fusion oncoprotein serves as a scaffold protein to bridge the *Groucho* corepressor TLE1 to transcription factor ATF2 in synovial sarcoma (Figure 3G).

Recent studies have identified the tumor suppressor *Early Growth Response 1* (*EGR1*) as a direct target of SS18-SSX (Lubieniecka et al., 2008). This gene was used to study the mechanisms underlying SS18-SSX occupancy of its targets. Chromatin IP (ChIP) with antibodies to ATF2, TLE1 and SS18-SSX identifies a common occupied DNA region around 100 bp upstream of the transcription start site of the human *EGR1* locus (Figure 4A). Sequence analysis of this promoter area reveals a consensus CRE site (5'-TCACGTCA-3'), which has been well defined in previous studies as a putative ATF2-binding element, and is phylogenetically conserved across diverse species (Faour et al., 2005; Hayakawa et al., 2004). This indicates that the transcription factor ATF2 may have a critical role in the recruitment of the SS18-SSX complex to target promoters. To test this possibility, we first examined the ATF2 cellular location because ATF2 has been shown to dynamically shuttle between the nucleus and cytoplasm in a context-dependent manner (Bhoumik et al., 2008; Liu et al., 2006; Maekawa et al., 2007). Immunohistochemical and immunofluorescent analysis of ATF2 in patient synovial sarcoma specimens and SYO-1 cells, respectively, shows that ATF2 is predominantly located in the nucleus (Figures 4B and 4C).

To examine the transcriptional activity of ATF2, published and in-house microarray expression profiles of patient specimens were interrogated (Baird et al., 2005; Nakayama et al., 2010; Nielsen et al., 2002) for the expression of known ATF2 target genes. In addition to two known SS18-SSX targets *EGR1* and *Nuclear Protein 1* (*NUPR1*, or *Candidate of Metastasis 1*, *COM1*) (Ishida et al., 2007), a set of seven more genes (Figure 5A) was chosen for further investigation because their promoters contain validated CRE sites for ATF2 binding (Figure S4A) (Hayakawa et al., 2004). These CRE sites are also conserved between humans and mice, and their protein products are involved in controlling cell cycle, apoptosis, and other cellular signalling pathways (Lopez-Bergami et al., 2010). To validate these candidate genes, ChIP was performed on *SS18-SSX1*- and *SS18-SSX2*-positive clinical tumor frozen tissue specimens. Site-specific qPCR shows both SS18-SSX1 and -SSX2 fusion proteins, together with ATF2 and TLE1, bind to the CRE-containing regions (Figures 5B and 5C, and Figures S4B and S4C). However, we were unable to detect any non-specific recruitment of these factors (Figures 5B and 5C, and Figures S4B and S4C), implying a possible predominant role for the ATF2-binding element in directing SS18-SSX promoter occupancy. To further evaluate SS18-SSX DNA binding activity, nuclear proteins were extracted from HEK293 stable cell lines with and without the fusion oncoprotein and incubated with infrared dye-labeled CRE oligonucleotides. An electrophoretic mobility shift assay (EMSA) identifies a specific protein-DNA complex, which is supershifted by the antibody against Myc-tag in Myc-SS18-SSX2-expressing cells, but not in control cells (Figure 5D). Consistently, a similar protein-DNA complex is also observed in human SYO-1 cells where it is supershifted by the antibodies to SS18-SSX, ATF2 and TLE1 (Figure 5E).

To further establish a direct link between ATF2 and recruitment of SS18-SSX, we used a specific siRNA to reduce the expression of ATF2 in human SYO-1 cells (Figure S5A). ChIP analyses reveal that loss of ATF2 significantly compromises the association of SS18-SSX2 and TLE1 with target gene promoters (Figure 6A). Furthermore, RT-qPCR analysis shows that transcript abundance of multiple ATF2 targets is increased after depleting ATF2 or SS18-SSX2 (Figure 6B). Consistent with this, in the mouse model of synovial sarcoma,

SS18-SSX2 and TLE1 binding to target gene promoters is abrogated after ATF2 depletion (Figure 6C and Figure S5B). Notably, an increased transcript level of either *Egr1* or *Atf3* was also observed in mATF2- and SS18-SSX2-knockdown mouse synovial sarcoma cells (Figure 6D). To confirm the specificity of this effect, wild-type (*wt*) or dominant-negative (*dn*) ATF2 was transfected into HEK293 cells in the presence or absence of the fusion protein SS18-SSX2. As shown in Figure S5C, compared with the *dn* form, overexpression of *wt* ATF2 in control cells significantly increases *EGR1* and *ATF3* transcript levels. However, this effect is no longer observed in *SS18-SSX2*-expressing cells, indicating in the presence of SS18-SSX2 ATF2 transactivational activity is reduced. In agreement with the RT-qPCR data, transfection of an *ATF3* reporter gene in human SYO-1 cells shows that the promoter activity for this ATF2 target gene is increased ~ 4-fold after *SS18-SSX2* depletion, while this stimulation is not seen in a construct with two point mutations in the CRE site of the *ATF3* promoter (Figure 6E). Thus, these experiments demonstrate that the SS18-SSX complex occupies ATF2 target genes and this is dependent upon its interaction with ATF2.

TLE1 also appears to be a functionally-important component of the SS18-SSX complex (Figures 2A, 2B and 2C). To assess whether TLE1 influences SS18-SSX transcriptional activity, TLE1 was knocked down in synovial sarcoma cells. Unlike ATF2 knockdown, depletion of TLE1 affects neither SS18-SSX2 nor ATF2 recruitment to target promoters *EGR1* and *ATF3* (Figure 7A). However, a significant increase in transcript levels for both tested target genes is detected by RT-qPCR in TLE1 knockdown cells, compared to control cells (Figure 7B). The specificity of this effect was further confirmed by showing that TLE1 depletion only induces *EGR1* and *ATF3* transcription in HEK293 cells in the presence of Myc-SS18-SSX2 (Figures S6A and S6B). These results indicate that SS18-SSX negatively regulates the transcription of its target genes via collaborating with TLE1. To gain molecular insights into the role of TLE1 in SS18-SSX-mediated repression, histone modifications were analyzed as previous work linked SS18-SSX recruitment to histone H3 lysine 27 trimethylation (H3K27me3), a key mark of gene repression (Lopez-Bergami et al., 2010). *TLE1* knockdown in SYO-1 cells results in a pronounced reduction in H3K27me3 levels at the same *EGR1* and *ATF3* promoter regions occupied by SS18-SSX, whereas the levels of trimethylated histone H3 at lysine 4 (H3K4me3), used as controls, are unchanged (Figure 7C). Given that H3K27me3 is a hallmark of PcG-dependent gene silencing (Cao et al., 2002; Muller et al., 2002), we asked whether TLE1 serves to link the PcG complex to SS18-SSX, thereby promoting repression of target genes. TLE1 has previously been shown to have a close relationship with the catalytic subunits of the PcG complex (Chen et al., 1999; Dasen et al., 2001; Higa et al., 2006). To test this directly in synovial sarcoma, human SYO-1 and primary SS18-SSX2 mouse model tumor cells were used for reciprocal IP analysis. In both cases, co-precipitation of TLE1 leads to enrichment of the PcG component, enhancer of zeste 2 (EZH2), and its functional co-factor, histone deacetylase 1 (HDAC1) (Figure S6C). Similar interactions were obtained with other core PcG subunits, such as the embryonic ectoderm development (EED) protein and suppressor of zeste 12 homolog (SUZ12) (Figures S6D and S6E). These same components of the HDAC/PcG complex had also been identified in mass spectrometric analysis of SS18-SSX2 enriched proteins (Figure S1C), and not surprisingly, EZH2 interactions are maintained in the absence of ATF2, but require TLE1 (Figure 7D). Consistent with these findings, ChIP analysis demonstrates that depletion of TLE1 is associated with a concomitant decrease in HDAC1 and EZH2 occupancy on both *EGR1* and *ATF3* target promoter regions (Figure 7E), suggesting that TLE1 functionally regulates HDAC/PcG recruitment to SS18-SSX target promoters. Reciprocal IP of TLE1, HDAC1, and EZH2 in normal human and mouse fibroblast cells (CCL153 and NIH/3T3) shows association of these three proteins (Figure 7F), and also raises the possibility that TLE1-containing complexes are shared between cancerous and normal cells. In accordance with observations in human tumor cells, TLE1 also has a critical role in assembling HDAC1 and EZH2 into the SS18-SSX complex and maintaining H3K27me3 levels and

transcriptional repression on the SS18-SSX-bound promoter regions in the mouse synovial sarcoma model (Figures 7G, 7H and 7I, and S6F). Taken together, these results indicate that TLE1 is responsible for SS18-SSX-mediated gene silencing by an HDAC/PcG-directed epigenetic mechanism.

The involvement of HDAC/PcG components in the repressor activity of the SS18-SSX complex suggests that HDAC or PcG proteins could be therapeutic targets for the treatment of synovial sarcoma. Indeed, it has been shown that repression of HDAC activity by small-molecule inhibitors can effectively suppress synovial sarcoma by reversing SS18-SSX-mediated epigenetic silencing (Lubieniecka et al., 2008; Su et al., 2010). To further examine the importance of HDAC proteins in regulating SS18-SSX activity, HDAC1 (identified as a core SS18-SSX complex subunit, Figure S1C) was knocked down. Similar to the published effects of HDAC inhibitors, depletion of HDAC1 from SYO-1 cells results in *EGR1* reactivation (Figure S7A), and is also associated with decreased cell growth and increased cell death (Figures S7B and S7C). Transcript levels for the SS18-SSX target genes *EGR1* and *ATF3*, as well as other identified targets, increase following addition of romidepsin or SB939 (clinical-grade HDAC inhibitors) (Figure 8A and Figure S7D). H3K27me3 repressive marks are decreased on the *EGR1* and *ATF3* promoters during HDAC inhibitor treatment (Figure 8B). Further analysis under the same conditions reveals a concomitant reduction in localization of HDAC1 and EZH2 to these ATF2 target promoters, even though their protein levels are unaffected (Figure 8B and Figure S7E). Consistent with this observation, HDAC inhibitor treatment of SYO-1 cells reduces HDAC1 and EZH2 appearance in the SS18-SSX complex (Figure 8C). Interestingly, HDAC1 and EZH2 remain bound to TLE1 before and after exposure to romidepsin (Figure S7F). As noted above, HDAC/PcG components are recruited to SS18-SSX through TLE1 (Figures 7D and 7E), and we thus hypothesized that HDAC inhibitors block HDAC/PcG activity by altering the behaviour of TLE1. In support of this possibility, glycerol-gradient sedimentation was performed using vehicle (DMSO)- or romidepsin-treated SYO-1 cell extracts. Western blot analysis shows that SS18-SSX2 and TLE1 are located in two separate elution peaks after HDAC inhibitor treatment, whereas the co-elution of ATF2 with the fusion protein appears to be stable under both conditions (Figure 8D). To directly test the effect of HDAC inhibitors on TLE1 recruitment, the interaction of TLE1 with SS18-SSX was assessed in the presence of romidepsin or SB939 (Figure 8C). Under these conditions, both HDAC inhibitors block the association of TLE1 with SS18-SSX and its DNA-binding partner ATF2. ChIP analysis in HDAC inhibitor-treated SYO-1 cells demonstrates the removal of TLE1 from target promoters while SS18-SSX2 and ATF2 remain resident (Figure S7G). A similar abrogation of TLE1, HDAC1, and EZH2 occupancy on the *Egr1* and *Atf3* promoters is observed in mouse synovial sarcoma cells following HDAC inhibitor treatment (Figure 8E). Congruent with this, romidepsin and SB939 induce a time-dependent increase in the expression of both *Egr1* and *Atf3* (Figure 8F), in accordance with a significant decrease in H3K27me3 levels on their promoter regions (Figure 8E). Taken together, these findings suggest that HDAC inhibitors derepress SS18-SSX target genes, at least in part through disrupting the recruitment of TLE1 and its associated HDAC/PcG proteins to the SS18-SSX complex, thus leading to loss of the repressive H3K27me3 mark and restored gene expression.

DISCUSSION

The nature through which SS18-SSX dysregulates transcription is a long-standing question in the synovial sarcoma field. Previous studies have shown that SS18-SSX can interact with components of the TrxG transcriptional activator complexes (Nagai et al., 2001; Thaete et al., 1999), as well it has been found to co-localize with PcG repressor factors (Soulez et al., 1999). Although these observations suggest a potential role for chromatin remodeling in

SS18-SSX-mediated gene silencing, it remained unclear how SS18-SSX controls the TrxG-PcG balance and, more importantly, how this fusion oncoprotein regulates gene expression in the absence of any known DNA-binding domain. In this study, we identify a core SS18-SSX transcriptional complex that is required for epigenetic silencing of tumor suppressor genes in synovial sarcoma. For assembly of this complex, the SS18-SSX fusion oncoprotein serves as a scaffolding protein to connect together two important transcriptional regulators, ATF2 and TLE1. SS18-SSX alone cannot bind to DNA, and its recruitment to target promoters is dependent on the sequence-specific transcriptional activator ATF2. In this manner, SS18-SSX recruitment of a TLE1-containing repressor complex functions to silence ATF2 target genes.

Modulation of ATF2 has also been identified in other cancers and interestingly, both activation and inhibition of ATF2 have been linked to tumorigenesis indicating that ATF2 function in cancer is context-dependent (Lopez-Bergami et al., 2010). For instance, in melanoma, activation of ATF2 which is associated with predominantly nuclear localization appears to be important for tumorigenesis and metastasis, while suppression of ATF2 leads to increased susceptability to various cell stressors. Conversely, in other cancers, loss or decreased expression of ATF2 is associated with an increased incidence of tumorgenesis and metastasis (Maekawa et al., 2008; Maekawa et al., 2007). Putative *ATF2* inactivating mutations in lung cancer have been identified, and in melanoma increased ATF2 cytoplasmic localization is associated with reduced tumorgenic potential and a better prognosis (Berger et al., 2003; Woo et al., 2002). *Atf2* heterozygous mice exhibit an increased incidence of breast cancer after a long latency period (> 60 weeks) suggesting that an additional hit(s) is required for tumor progression in this background (Maekawa et al., 2007). However, this second hit may in part involve loss of ATF2, as in all tumors examined ATF2 was undetectable. In a skin cancer model in mice, deletion of *Atf2* was sufficient to increase the appearance of precancerous lesions (Bhoumik et al., 2008). However, in this model loss of ATF2 appears to promote tumorgenesis and is unlikely involved in initation. Together, these studies support a fundamental role for ATF2 in tumorgenesis, and highlight the varied mechanisms employed to inactivate its function.

In synovial sarcoma ATF2 function is disrupted through a mechanism in which the fusion oncoprotein couples ATF2 to a TLE1-containing complex. Interestingly, while ATF2 shows predominantly nuclear localization, the presence of the fusion oncoprotein in turn leads to repression of ATF2 target genes. Repression of ATF2 targets is observed in both synovial sarcoma-derived cell lines and in primary tumors. Furthermore, restoration of ATF2 transcriptional activity and/or the expression of some ATF2 target genes leads to growth suppression and apoptosis in synovial sarcoma cells, indicating that loss of ATF2 function is important for the maintenance of the tumor cell phenotype. Importantly, loss of TLE1 phenocopies loss of ATF2, and leads to up-regulation of several ATF2 target genes. In this regard, TLE1 appears to function in a dominant-negative manner on ATF2-mediated transactivation, by mediating HDAC/PcG-directed gene silencing of ATF2 targets. It should be noted that TLE1 expression is an important clinical feature for distinguishing synovial sarcoma from other soft-tissue tumors (Jagdis et al., 2009; Knosel et al., 2010; Terry et al., 2007). However, the relevance of TLE1 as a specific biomarker for this disease remains controversial (Foo et al., 2011; Kosemehmetoglu et al., 2009), in part due to an absence of supportive functional data. Herein, we define a fundamental role for TLE1 in the etiology of synovial sarcoma and provide a biological rationale for its use as a diagnostic biomarker and potential therapeutic target in synovial sarcoma.

Synovial sarcomas have been shown to be highly sensitive to HDAC inhibitors in preclinical models (Ito et al., 2005; Liu et al., 2008), and herein we find that the interaction between SS18-SSX and TLE1 is critical in regulating the epigentic reprogramming that occurs

following HDAC inhibitor treatment. Based on these findings, we propose a model (Figure 8G) wherein HDAC inhibitors relieve SS18-SSX-mediated repression at ATF2 target genes most likely through removal of TLE1 and its associated HDAC/PcG factors from SS18-SSX. Consequently, as was also observed with TLE1 knockdown, HDAC/PcG complexes are no longer recruited to ATF2 target promoters. In support of this concept, TLE1 depletion similarly results in diminished H3K27me3 signals and elevated transcript levels for ATF2/SS18-SSX target genes. The mechanisms underlying HDAC inhibitor induced disruption of SS18-SSX-TLE1 interaction are currently unknown, but are being investigated. In summary, our findings provide fundamental insights into the nature of the SS18-SSX transcriptional complex, including a DNA-binding partner protein (ATF2) and abnormal recruitment of enzymatic epigenetic corepressors via TLE1. This information provides a biological rationale for including synovial sarcoma in clinical trials of HDAC inhibitors (NCT01112384, NCT00918489, NCT00878800) and a framework for identifying therapeutic strategies to treat this deadly disease.

EXPERIMENTAL PROCEDURES

Cells, Tissues and Chemicals

Human synovial sarcoma cell lines SYO-1 and FUJI were kindly provided by Dr. Akira Kawai (National Cancer Centre Hospital, Tokyo, Japan) and Dr. Kazuo Nagashima (Hokkaido University School of Medicine, Sapporo, Japan) and maintained in RPMI-1640 medium with 10% fetal bovine serum (FBS) (Invitrogen). Human embryonic kidney HEK293 cells stably expressing Myc-tagged SS18 or SS18-SSX2 were grown in DMEM medium with 10% FBS and 400ug/ml Zeocin (Invitrogen). Primary mouse synovial sarcoma cells were isolated from tumors of female *Myf5-Cre/SSM2* mice as described previously (Haldar et al., 2007), and cultured in DMEM medium with 10% FBS. All cells were maintained at 37°C, 95% humidity, and 5% CO_2.

Human subjects in this study provided informed consent for use of tissues for research purposes following procedures approved by the Clinical Research Ethics Board of the University of British Columbia (projects H08-0717 "Sarcoma tissue bank" and H06-00013 "Molecular targets for therapy of sarcoma")

HDAC inhibitors romidepsin (FK228, Depsipeptide, or NSC-630176) and SB939 were obtained from the Developmental Therapeutic Branch of the National Cancer Institute (Bethesda, MD, USA) and S*BIO Pte Ltd (Singapore), respectively. DMSO was purchased from Sigma-Aldrich.

Plasmid DNA Constructs

To define the domains within SS18-SSX2 that interact with ATF2 and TLE1, variants missing the SNH or QPGY domain of SS18 and the SSXRD domain of SSX2 were generated via gene synthesis (Integrated DNA Technologies) and sub-cloned as EcoR1 – Not1 fragments into the mammalian expression vector pcDNA4/myc-HisA (Life Technologies). All genes were engineered to remove the stop, allowing read-through to generate a C-terminal Myc-6XHis tag.

Immunoprecipitation (IP) and Western Blots

For immunoprecipitation, cells were washed twice with ice-cold PBS, and incubated with RIPA buffer (Santa Cruz Biotechnology) for 35 min on ice. Whole cell lysates were centrifuged at 4°C, at full speed in a microcentrifuge for 15 min, and the supernatants were mixed with 15 ul of protein A/G agarose beads (Santa Cruz Biotechnology) for 45 min at 4°C for pre-clearing. For immunoprecipitation, 500 ug of pre-cleared proteins were

incubated with 1.5 ug of indicated antibody at 4°C overnight, followed by the addition of 25 ul of protein A/G agarose beads. After a 3-hr incubation at 4°C, the beads were precipitated, washed once with RIPA buffer and twice with ice-cold PBS, and boiled in 2×loading dye for 5 min. Samples were separated by 10–12% sodium dodecyl sulfate-polyacrylamide gel eletrophoresis (SDS-PAGE), and transferred to nitrocellulose membranes (Bio-Rad Laboratories). Blots were incubated with indicated antibodies (see below for details). Signals were visualized using the Odyssey Infrared System (LI-COR Biosciences).

Mass Spectrometry

Coomassie blue stained bands were excised from the gel and reduced with dithiothreitol (DTT), followed by alkylation with iodoacetamide (IAA). Gel bands were digested with Trypsin at 37°C overnight as described (Shevchenko et al., 1996). Proteolytically digested peptides were then extracted from the gel pieces, reconstituted in formic acid (FA), and analyzed on a QStar XL LC-MS/MS (Applied Biosystems). The MS/MS peaks were submitted to Mascot and gpmDB for peptide sequence database search (Wong et al., 2009). Both of these databases were employed to confirm peptide/protein identification in this study.

Immunofluorescence and Immunohistochemistry

SYO-1 cells were cultured on glass coverslips, fixed with 3:1 acetone-methanol at −20°C for 7 min, and blocked with 5% bovine serum albumin (BSA) for 30 min. Cells were then incubated with a polyclonal ATF2 rabbit antibody (Santa Cruz Biotechnology) at 4°C overnight, followed by three washes with ice-cold PBS. After incubation with AlexFluor Conjugated anti-Rabbit secondary antibody (New England Biolabs), the coverslips were mounted in 50% glycerol and 2% DABCO (Sigma-Aldrich). The cellular localization of ATF2 was analysed under a fluorescence microscope (Zeiss).

Primary synovial sarcoma, malignant peripheral nerve sheath and breast cancer samples were embedded in paraffin, and stained with the same ATF2 antibody used in immunofluorescence. All immunostainings were performed with avidin-biotin-peroxidase complex technique (VectaStain) in combination with diaminobenzidine (DAB), and counterstained with hematoxylin and eosin (H&E) on surgical pathology specimens as described previously (Pacheco et al., 2010; Terry et al., 2007). Negative controls were carried out with rabbit IgG.

Glycerol-Gradient Sedimentation

Nuclear extracts were prepared from SYO-1 and HEK293 stable cell lines using the Pierce NE-PER Nuclear Extraction kit. Samples were then subjected to a 10%–40% glycerol gradient in 4.8 ml buffer (150 mM NaCl, 10 mM HEPES (pH 7.5), 2 mM DTT, 1 mM EDTA, and 0.1% Triton X-100), and centrifuged at 40,000 rpm for 16 hr at 4°C in a SW50.1 rotor (Beckman). Fractions (160 ul) were collected starting from the top of the gradient, followed by SDS-PAGE and western blot analysis. To determine molecular weight of fractions, marker proteins thyroglobulin (M. Wt. 669 kDa), β-amylase (M.Wt. 200 kDa) and bovine serum albumin (M.Wt. 66 kDa) were spiked into the gradients and detected using their respective antibodies.

RNA Interference (RNAi)

The small interfering RNAs (siRNAs) specific for ATF2/mATF2, TLE1/mTLE1, and HDAC1 were purchased from Dharmacon and Santa Cruz Biotechnology, respectively. Two different SS18-SSX2 siRNAs were synthesized by Integrated DNA Technologies (IDT) as described in previous studies (Garcia et al., 2011; Lubieniecka et al., 2008). At 60%

confluence, cells were transfected with the indicated siRNA using Lipofectamine RNAiMAX transfection reagent (Invitrogen) according to the manufacturer's instructions. Except where indicated, lysates or RNA were harvested 48 hr post-transfection, and used for IP, glycerol gradients, reporter gene assays, RT-qPCR and western blots. Knockdown efficiency was determined by RT-qPCR.

Cell Growth and Colony Formation Assay

To measure cell growth rate, human and mouse synovial sarcoma cells were cultured at 60% confluence on 48-well plates, and transfected with the indicated siRNA using Lipofectamine RNAiMAX transfection reagent (Invitrogen). At various times after transfection, cell growth was monitored by MTT assay (Life Technologies), and normalized to control cells to give relative growth rate of cells. For colony formation assay, control and knockdown cells were replated on 6-well plates at a density of 1×10^3 cells per well. After 8 days of incubation, cells were fixed with 10% formalin and stained with 0.1% crystal violet, and the colonies counted by using Image J software as described (Junttila et al., 2007).

Cell Death and Apoptosis Assay

Cells were cultured with propidium iodide (PI) at a concentration of 500 ng/ml, followed by transfection with the indicated siRNA. Cell death was indicated by PI-positive cells, and visualized under a fluorescence microscope (Zeiss). For analysis of apoptosis, cells were harvested 72 hr post siRNA transfection, and suspended in Annexin-V-FITC-PI dye (Invitrogen). After adding Annexin-V binding buffer, the samples were run through a FACS scan flow cytometer (Becton Dickinson) as described (Kawase et al., 2009). Summit for MoFlo Acquisition and Sort Control Software was used to quantify apoptosis (Annexin-V positive cells).

Chromatin Immunoprecipitation (ChIP)

ChIP experiments were performed following the Active Motif protocol as described (Su et al., 2010). Briefly, 5×10^7 cells or 150 mg synovial sarcoma tissues were cross-linked with 1% formaldehyde prior to lysis and homogenization. Cross-linked DNA was sheared using a Bioruptor-UCD300 sonicator (Diagenode) for 15 × 25 second pulses (60 second pause between pulses) at 4°C. After centrifugation, the supernatants were pre-cleared with Protein G beads for 30 min at 4°C, and incubated with the indicated antibody at 4°C overnight. After 4-hr incubation with Protein G beads, the precipitates were washed four times with different washing buffers (Active Motif), eluted with 1% SDS, and incubated at 65°C overnight to reverse cross-linking. ChIP-enriched DNA was purified using the Qiagen PCR Purification kit, and subjected to SYBR Green qPCR analysis (Roche) using various primer sets (supplemental information).

Electrophoretic Mobility Shift Assay (EMSA)

The *ATF/CRE* probe was purchased from LI-COR, and labeled on the 5'-end of each strand with Infrared Dye-700nm. The wild-type and mutant *ATF/CRE* competitor probes were obtained from Santa Cruz Biotechnology. Binding reactions were peformed in the dark at room temperature for 30 min in 25 ul of EMSA buffer (250 mM NaCl, 20 mM HEPES (pH 7.9), 2 mM DTT, 20% glycerol, 0.5% Tween 20) as described before (Boyle et al., 2009). Samples were separated on 4% polyacrylamide gels (29.2:0.8 acrylamide-bisacrylamide in 100 mM Tris, 100 mM borate, and 10 mM EDTA). The extent of gel shift was then visualized on the Odyssey Infrared scanner (LI-COR).

Luciferase Reporter Assay

For luciferase reporter assays, transient transfections were performed using FuGENE 6 transfection reagent (Roche). SYO-1 cells were subcultured in 24-well plates, and transfected with the wild-type or mutant human *ATF3* promoter-firefly luciferase reporter plasmid together with renilla luciferase expression vector. After 24-hr incubation, the control or SS18-SSX2-specific siRNA was introduced using Lipofectamine RNAiMAX transfection reagent (Invitrogen). Cells were harvested at 48 hrs post siRNA transfection, and analyzed using the Dual-Luciferase Reporter Assay system (Promega). Firefly luciferase was normalized to renilla luciferase activity to control for differences in transfection efficiency and to generate relative luciferase activity.

Real-time quantitative PCR

Total RNA was isolated and then transcribed to cDNA using the Qiagen RNeasy Mini kit and the high-capacity cDNA reverse transcription kit (Applied Biosystems), respectively, as described previously (Su et al., 2010). Taqman gene expression assays were performed by using the ABI-7500 Fast Real-Time PCR System with specific primer/probe sets (Applied Biosystems). All transcript levels were normalized to 18s ribosomal (rRNA) expression.

Antibodies

The rabbit polyclonal antibody (RA2009) against SS18-SSX was kindly provided by Dr. Diederik R.H. de Bruijn (Radbound University Nijmegen Medical Centre, Nijmegen, the Netherlands). The antibodies for SS18 (H-80), SSX (C-9), ATF2 (C-19), TLE1 (M-101 and N-18), HDAC1 (10E2), β-Actin (N-21), Caspase-3 (H-277), and EGR1 (588) were purchased from Santa Cruz Biotechnology. The H3K4me3 (Upstate 05–745) and H3k27me3 (Upstate 07–449) antibodies were used for chromatin immunoprecipitation. For immunoprecipitation and western blots, we also used the following antibodies: Myc (Cell Signaling #2278), HDAC1 (Abcam ab1767), EZH2 (Active Motif #39639), EED (Abcam ab4469), SUZ12 (Abcam ab12073), Caspase-3 (Cell Signaling #9668), and GFP (Cell Signaling #2555).

Supplementary Material

Refer to Web version on PubMed Central for supplementary material.

Acknowledgments

We thank Dr. Diederik R.H. de Bruijn (Radbound University Nijmegen Medical Centre, Nijmegen, the Netherlands) for rabbit polyclonal antibody against SS18-SSX and enlightened discussion of SS18-SSX ChIP data, and Drs. Junya Kawauchi and Shigetaka Kitajima (Tokyo Medical and Dental University, Tokyo, Japan) for human *ATF3* promoter-luciferase reporter plasmids. Romidepsin was generously provided by Celgene Corporation (Gloucester Pharmaceuticals Inc.) and the National Cancer Institute and SB939 was provided by S*BIO Pte Ltd (Singapore). This work was supported by grants from the Canadian Cancer Society Research Institute (Grant #018355) and the Terry Fox Foundation and CIHR Institute of Cancer (TFF 105265). K.B.J. receives career development support from the National Cancer Institute (NIH) K08CA138764 and additional support from the Paul Nabil Bustany Fund for Synovial Sarcoma Research. T.O.N. is a Michael Smith Foundation of Health Research senior scholar.

REFERENCES

Ali SA, Zaidi SK, Dobson JR, Shakoori AR, Lian JB, Stein JL, van Wijnen AJ, Stein GS. Transcriptional corepressor TLE1 functions with Runx2 in epigenetic repression of ribosomal RNA genes. Proc Natl Acad Sci U S A. 2010; 107:4165–4169. [PubMed: 20160071]

Baird K, Davis S, Antonescu CR, Harper UL, Walker RL, Chen Y, Glatfelter AA, Duray PH, Meltzer PS. Gene expression profiling of human sarcomas: insights into sarcoma biology. Cancer Res. 2005; 65:9226–9235. [PubMed: 16230383]

Berger AJ, Kluger HM, Li N, Kielhorn E, Halaban R, Ronai Z, Rimm DL. Subcellular localization of activating transcription factor 2 in melanoma specimens predicts patient survival. Cancer Res. 2003; 63:8103–8107. [PubMed: 14678960]

Bhoumik A, Fichtman B, Derossi C, Breitwieser W, Kluger HM, Davis S, Subtil A, Meltzer P, Krajewski S, Jones N, Ronai Z. Suppressor role of activating transcription factor 2 (ATF2) in skin cancer. Proc Natl Acad Sci U S A. 2008; 105:1674–1679. [PubMed: 18227516]

Boyle P, Le Su E, Rochon A, Shearer HL, Murmu J, Chu JY, Fobert PR, Despres C. The BTB/POZ domain of the Arabidopsis disease resistance protein NPR1 interacts with the repression domain of TGA2 to negate its function. Plant Cell. 2009; 21:3700–3713. [PubMed: 19915088]

Cao R, Wang L, Wang H, Xia L, Erdjument-Bromage H, Tempst P, Jones RS, Zhang Y. Role of histone H3 lysine 27 methylation in Polycomb-group silencing. Science. 2002; 298:1039–1043. [PubMed: 12351676]

Chen G, Fernandez J, Mische S, Courey AJ. A functional interaction between the histone deacetylase Rpd3 and the corepressor groucho in Drosophila development. Genes Dev. 1999; 13:2218–2230. [PubMed: 10485845]

Dasen JS, Barbera JP, Herman TS, Connell SO, Olson L, Ju B, Tollkuhn J, Baek SH, Rose DW, Rosenfeld MG. Temporal regulation of a paired-like homeodomain repressor/TLE corepressor complex and a related activator is required for pituitary organogenesis. Genes Dev. 2001; 15:3193–3207. [PubMed: 11731482]

de Bruijn DR, Allander SV, van Dijk AH, Willemse MP, Thijssen J, van Groningen JJ, Meltzer PS, van Kessel AG. The synovial-sarcoma-associated SS18-SSX2 fusion protein induces epigenetic gene (de)regulation. Cancer Res. 2006; 66:9474–9482. [PubMed: 17018603]

Faour WH, Alaaeddine N, Mancini A, He QW, Jovanovic D, Di Battista JA. Early growth response factor-1 mediates prostaglandin E2-dependent transcriptional suppression of cytokine-induced tumor necrosis factor-alpha gene expression in human macrophages and rheumatoid arthritis-affected synovial fibroblasts. J Biol Chem. 2005; 280:9536–9546. [PubMed: 15640148]

Foo WC, Cruise MW, Wick MR, Hornick JL. Immunohistochemical staining for TLE1 distinguishes synovial sarcoma from histologic mimics. Am J Clin Pathol. 2011; 135:839–844. [PubMed: 21571956]

Haldar M, Hancock JD, Coffin CM, Lessnick SL, Capecchi MR. A conditional mouse model of synovial sarcoma: insights into a myogenic origin. Cancer Cell. 2007; 11:375–388. [PubMed: 17418413]

Haldar M, Randall RL, Capecchi MR. Synovial sarcoma: from genetics to genetic-based animal modeling. Clin Orthop Relat Res. 2008; 466:2156–2167. [PubMed: 18563504]

Hayakawa J, Mittal S, Wang Y, Korkmaz KS, Adamson E, English C, Ohmichi M, McClelland M, Mercola D. Identification of promoters bound by c-Jun/ATF2 during rapid large-scale gene activation following genotoxic stress. Mol Cell. 2004; 16:521–535. [PubMed: 15546613]

Higa LA, Wu M, Ye T, Kobayashi R, Sun H, Zhang H. CUL4-DDB1 ubiquitin ligase interacts with multiple WD40-repeat proteins and regulates histone methylation. Nat Cell Biol. 2006; 8:1277–1283. [PubMed: 17041588]

Ishida M, Miyamoto M, Naitoh S, Tatsuda D, Hasegawa T, Nemoto T, Yokozeki H, Nishioka K, Matsukage A, Ohki M, Ohta T. The SYT-SSX fusion protein down-regulates the cell proliferation regulator COM1 in t(x;18) synovial sarcoma. Mol Cell Biol. 2007; 27:1348–1355. [PubMed: 17101797]

Ito T, Ouchida M, Morimoto Y, Yoshida A, Jitsumori Y, Ozaki T, Sonobe H, Inoue H, Shimizu K. Significant growth suppression of synovial sarcomas by the histone deacetylase inhibitor FK228 in vitro and in vivo. Cancer Lett. 2005; 224:311–319. [PubMed: 15914281]

Jagdis A, Rubin BP, Tubbs RR, Pacheco M, Nielsen TO. Prospective evaluation of TLE1 as a diagnostic immunohistochemical marker in synovial sarcoma. Am J Surg Pathol. 2009; 33:1743–1751. [PubMed: 19809272]

Junttila MR, Puustinen P, Niemela M, Ahola R, Arnold H, Bottzauw T, Ala-aho R, Nielsen C, Ivaska J, Taya Y, et al. CIP2A inhibits PP2A in human malignancies. Cell. 2007; 130:51–62. [PubMed: 17632056]

Kawasaki H, Schiltz L, Chiu R, Itakura K, Taira K, Nakatani Y, Yokoyama KK. ATF-2 has intrinsic histone acetyltransferase activity which is modulated by phosphorylation. Nature. 2000; 405:195–200. [PubMed: 10821277]

Kawase T, Ohki R, Shibata T, Tsutsumi S, Kamimura N, Inazawa J, Ohta T, Ichikawa H, Aburatani H, Tashiro F, Taya Y. PH domain-only protein PHLDA3 is a p53-regulated repressor of Akt. Cell. 2009; 136:535–550. [PubMed: 19203586]

Knosel T, Heretsch S, Altendorf-Hofmann A, Richter P, Katenkamp K, Katenkamp D, Berndt A, Petersen I. TLE1 is a robust diagnostic biomarker for synovial sarcomas and correlates with t(X; 18): analysis of 319 cases. Eur J Cancer. 2010; 46:1170–1176. [PubMed: 20189377]

Kosemehmetoglu K, Vrana JA, Folpe AL. TLE1 expression is not specific for synovial sarcoma: a whole section study of 163 soft tissue and bone neoplasms. Mod Pathol. 2009; 22:872–878. [PubMed: 19363472]

Ladanyi M. Fusions of the SYT and SSX genes in synovial sarcoma. Oncogene. 2001; 20:5755–5762. [PubMed: 11607825]

Lim FL, Soulez M, Koczan D, Thiesen HJ, Knight JC. A KRAB-related domain and a novel transcription repression domain in proteins encoded by SSX genes that are disrupted in human sarcomas. Oncogene. 1998; 17:2013–2018. [PubMed: 9788446]

Liu H, Deng X, Shyu YJ, Li JJ, Taparowsky EJ, Hu CD. Mutual regulation of c-Jun and ATF2 by transcriptional activation and subcellular localization. EMBO J. 2006; 25:1058–1069. [PubMed: 16511568]

Liu S, Cheng H, Kwan W, Lubieniecka JM, Nielsen TO. Histone deacetylase inhibitors induce growth arrest, apoptosis, and differentiation in clear cell sarcoma models. Mol Cancer Ther. 2008; 7:1751–1761. [PubMed: 18566246]

Lopez-Bergami P, Lau E, Ronai Z. Emerging roles of ATF2 and the dynamic AP1 network in cancer. Nat Rev Cancer. 2010; 10:65–76. [PubMed: 20029425]

Lubieniecka JM, de Bruijn DR, Su L, van Dijk AH, Subramanian S, van de Rijn M, Poulin N, van Kessel AG, Nielsen TO. Histone deacetylase inhibitors reverse SS18-SSX-mediated polycomb silencing of the tumor suppressor early growth response 1 in synovial sarcoma. Cancer Res. 2008; 68:4303–4310. [PubMed: 18519690]

Maekawa T, Sano Y, Shinagawa T, Rahman Z, Sakuma T, Nomura S, Licht JD, Ishii S. ATF-2 controls transcription of Maspin and GADD45 alpha genes independently from p53 to suppress mammary tumors. Oncogene. 2008; 27:1045–1054. [PubMed: 17700520]

Maekawa T, Shinagawa T, Sano Y, Sakuma T, Nomura S, Nagasaki K, Miki Y, Saito-Ohara F, Inazawa J, Kohno T, et al. Reduced levels of ATF-2 predispose mice to mammary tumors. Mol Cell Biol. 2007; 27:1730–1744. [PubMed: 17189429]

Muller J, Hart CM, Francis NJ, Vargas ML, Sengupta A, Wild B, Miller EL, O'Connor MB, Kingston RE, Simon JA. Histone methyltransferase activity of a Drosophila Polycomb group repressor complex. Cell. 2002; 111:197–208. [PubMed: 12408864]

Nagai M, Tanaka S, Tsuda M, Endo S, Kato H, Sonobe H, Minami A, Hiraga H, Nishihara H, Sawa H, Nagashima K. Analysis of transforming activity of human synovial sarcoma-associated chimeric protein SYT-SSX1 bound to chromatin remodeling factor hBRM/hSNF2 alpha. Proc Natl Acad Sci U S A. 2001; 98:3843–3848. [PubMed: 11274403]

Nakayama R, Mitani S, Nakagawa T, Hasegawa T, Kawai A, Morioka H, Yabe H, Toyama Y, Ogose A, Toguchida J, et al. Gene expression profiling of synovial sarcoma: distinct signature of poorly differentiated type. Am J Surg Pathol. 2010; 34:1599–1607. [PubMed: 20975339]

Nielsen TO, West RB, Linn SC, Alter O, Knowling MA, O'Connell JX, Zhu S, Fero M, Sherlock G, Pollack JR, et al. Molecular characterisation of soft tissue tumours: a gene expression study. Lancet. 2002; 359:1301–1307. [PubMed: 11965276]

Pacheco M, Horsman DE, Hayes MM, Clarkson PW, Huwait H, Nielsen TO. Small blue round cell tumor of the interosseous membrane bearing a t(2;22)(q34;q12)/EWS-CREB1 translocation: a case report. Mol Cytogenet. 2010; 3:12. [PubMed: 20598147]

Shevchenko A, Jensen ON, Podtelejnikov AV, Sagliocco F, Wilm M, Vorm O, Mortensen P, Boucherie H, Mann M. Linking genome and proteome by mass spectrometry: large-scale identification of yeast proteins from two dimensional gels. Proc Natl Acad Sci U S A. 1996; 93:14440–14445. [PubMed: 8962070]

Soulez M, Saurin AJ, Freemont PS, Knight JC. SSX and the synovial-sarcoma-specific chimaeric protein SYT-SSX co-localize with the human Polycomb group complex. Oncogene. 1999; 18:2739–2746. [PubMed: 10348348]

Su L, Cheng H, Sampaio AV, Nielsen TO, Underhill TM. EGR1 reactivation by histone deacetylase inhibitors promotes synovial sarcoma cell death through the PTEN tumor suppressor. Oncogene. 2010; 29:4352–4361. [PubMed: 20514024]

Terry J, Saito T, Subramanian S, Ruttan C, Antonescu CR, Goldblum JR, Downs-Kelly E, Corless CL, Rubin BP, van de Rijn M, et al. TLE1 as a diagnostic immunohistochemical marker for synovial sarcoma emerging from gene expression profiling studies. Am J Surg Pathol. 2007; 31:240–246. [PubMed: 17255769]

Thaete C, Brett D, Monaghan P, Whitehouse S, Rennie G, Rayner E, Cooper CS, Goodwin G. Functional domains of the SYT and SYT-SSX synovial sarcoma translocation proteins and co-localization with the SNF protein BRM in the nucleus. Hum Mol Genet. 1999; 8:585–591. [PubMed: 10072425]

Wong JP, Reboul E, Molday RS, Kast J. A carboxy-terminal affinity tag for the purification and mass spectrometric characterization of integral membrane proteins. J Proteome Res. 2009; 8:2388–2396. [PubMed: 19236039]

Woo IS, Kohno T, Inoue K, Ishii S, Yokota J. Infrequent mutations of the activating transcription factor-2 gene in human lung cancer, neuroblastoma and breast cancer. Int J Oncol. 2002; 20:527–531. [PubMed: 11836564]

SIGNIFICANCE

Synovial sarcoma is a cancer of adolescents and young adults for which conventional chemotherapy has limited benefit and metastatic disease is usually fatal. Preclinical studies have shown sensitivity to HDAC inhibitors, which are being evaluated in clinical trials. However, the mechanistic basis of SS18-SSX-mediated tumorigenesis and HDAC inhibitor action in synovial sarcoma has not been defined. Herein we identify ATF2 as the DNA binding partner of SS18-SSX and show that HDAC inhibitors reverse the epigenetic repressor activity of the SS18-SSX oncoprotein complex by preventing TLE1 recruitment. These findings thus uncover a role for HDAC inhibitors in fusion oncoprotein complex assembly, and may inform concurrent investigations on other types of translocation-associated cancer.

HIGHLIGHTS

SS18-SSX interacts with ATF2 and TLE1 in human synovial sarcoma cells;

ATF2 recruits the SS18-SSX complex to specific gene promoters;

TLE1 is responsible for SS18-SSX-mediated repression of ATF2 targets;

HDAC inhibitors disrupt the SS18-SSX complex.

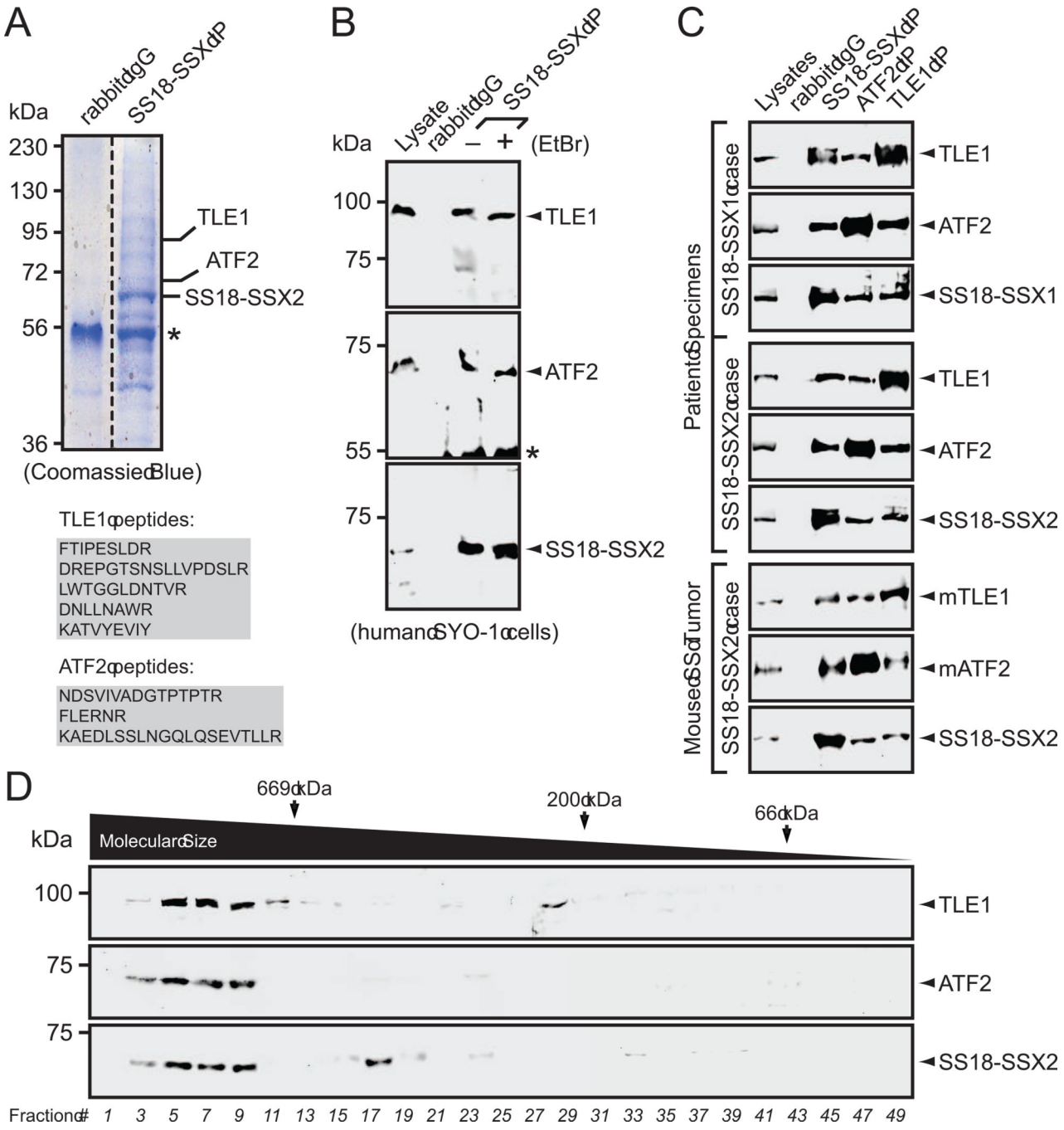

Figure 1. SS18-SSX associates with ATF2 and TLE1 in synovial sarcoma

(A) Coomassie-stained gel of the SS18-SSX complex in SYO-1 cells. ATF2 and TLE1 were identified by mass spectrometry. Asterisk indicates IgG bands.

(B) Western blot analysis of the SS18-SSX precipitates (in the presence or absence of ethidium bromide, EtBr) in SYO-1 cells. Rabbit IgG was used as a negative control.

(C) Reciprocal immunoprecipitation (IP) of SS18-SSX, ATF2, and TLE1 showing their interactions in human and mouse synovial sarcoma (SS) tumors.

(D) Glycerol-gradient fractionation profile of SS18-SSX2, ATF2 and TLE1 in SYO-1 cells. See also Figure S1.

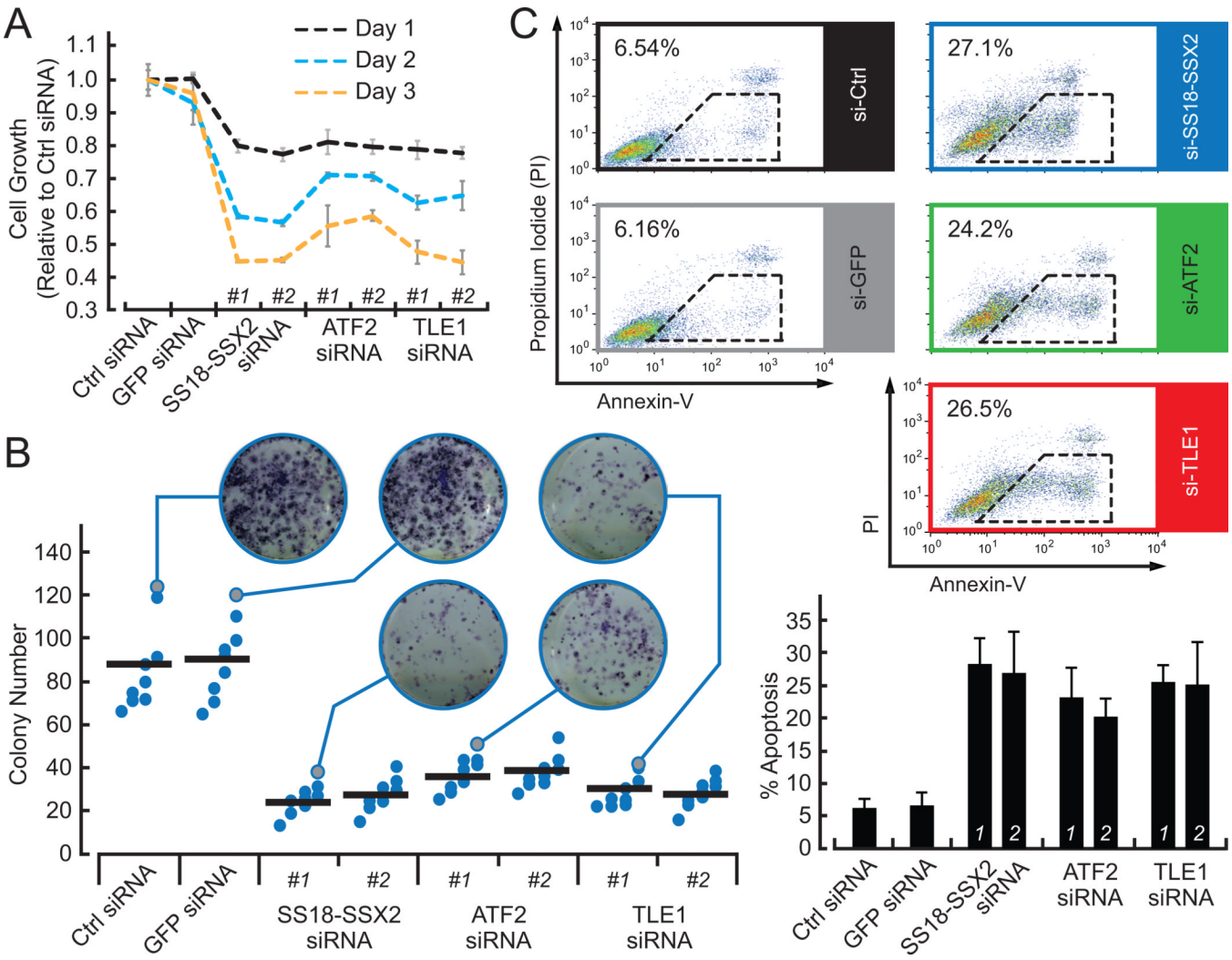

Figure 2. Disruption of the SS18-SSX complex reduces synovial sarcoma cell growth

(A) The effect of SS18-SSX2, ATF2 and TLE1 knockdown on SYO-1 cell growth. Data represent mean ±S.D. of three experiments.

(B) Colony formation assays on SYO-1 cells at 8 days after indicated siRNA transfections. Representative images for crystal violet stain, and quantitation of number of colonies by Image J software. The black bars represent the mean.

(C) Flow cytometric analysis of apoptotic SYO-1 cells transfected with indicated siRNA following 72 hr. Percentages of Annexin-V$^+$ cells are shown (n = 3). Bar charts are mean +/− SD. See also Figure S2.

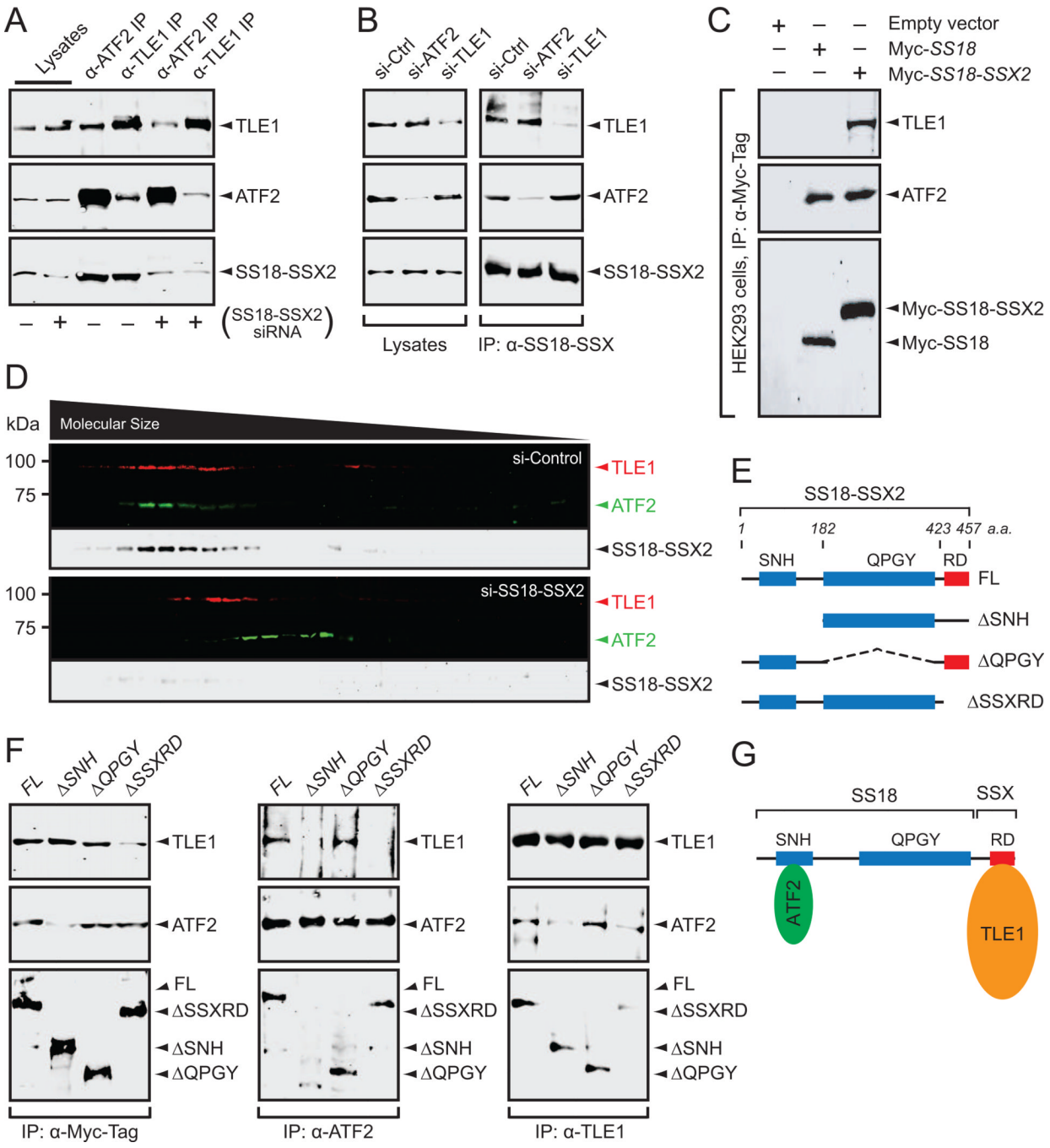

Figure 3. Molecular association of SS18-SSX with ATF2 and TLE1

(A) Reciprocal IP of ATF2 and TLE1 in control and SS18-SSX2 knockdown SYO-1 cells. Western blot analysis of whole cell lysates following SS18-SSX2 knockdown are shown on the left.

(B) Western blot analysis of the extracts of control, ATF2 and TLE1 knockdown SYO-1 cells immunoprecipitated by the anti-SS18-SSX antibody.

(C) Myc IP analysis of HEK293 cells stably expressing empty vector, Myc-tagged wild-type *SS18* or *SS18-SSX2*.

(D) Sedimentation profile of control and SS18-SSX2 knockdown SYO-1 cell extracts by 10–40% glycerol gradients.

(E) Schematic representing C-terminal Myc-tagged *SS18-SSX2* truncation and deletion constructs. FL, full-length fusion oncoprotein; SNH, SYT N-terminal homolog; QPGY, glycine-/proline-/glutamine-/tyrosine-domain; SSXRD, SSX repressor domain.
(F) Mapping the interface in SS18-SSX2 for its association with ATF2 and TLE1 by reciprocal IP experiments with the Myc, ATF2 and TLE1 antibodies in HEK293 cells expressing the SS18-SSX2 constructs as described in (E).
(G) Schematic model illustrating the scaffolding role of SS18-SSX in ATF2 and TLE1 association. See also Figure S3.

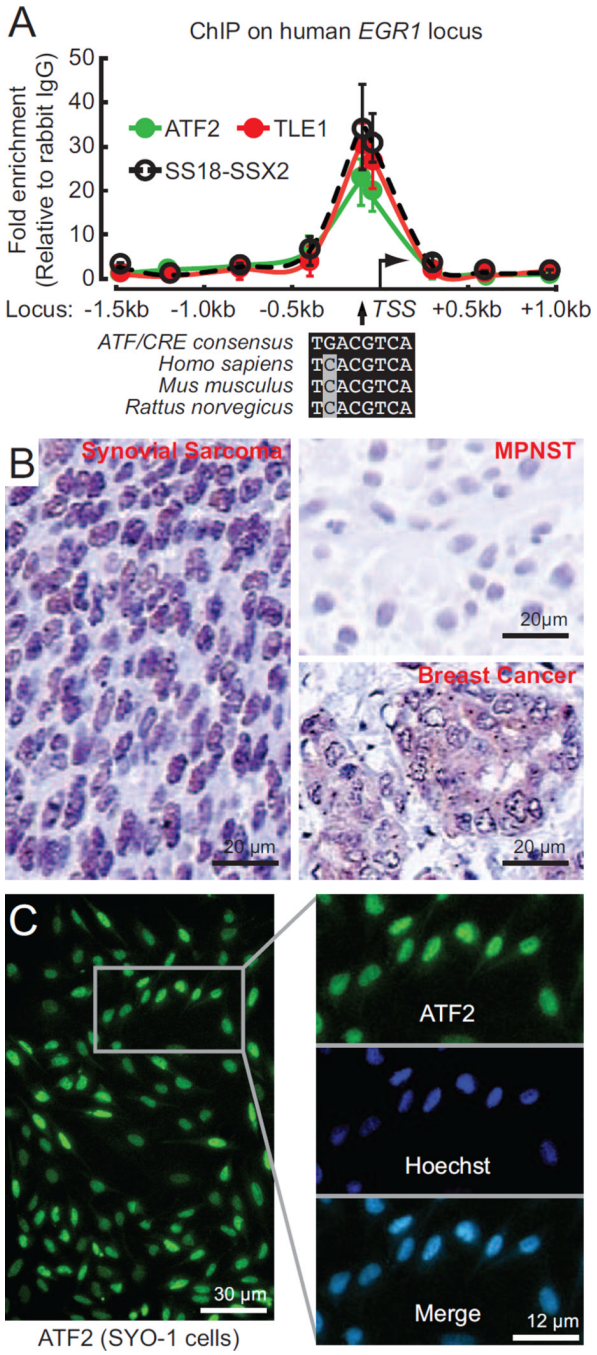

Figure 4. ATF2 is recruited to the *EGR1* promoter along with TLE1 and SS18-SSX, and is localized to the nucleus in synovial sarcoma

(A) Binding of SS18-SSX, ATF2, and TLE1 across the human *EGR1* locus was assessed by chromatin immunoprecipitation (ChIP) and site-specific qPCR. Data shown are the mean ±S.D. of three experiments where values are expressed relative to rabbit IgG.

(B) Endogenous ATF2 protein is localized to the nucleus in primary synovial sarcoma tissues by immunohistochemistry. Malignant peripheral nerve sheath tumor (MPNST) was used as a ATF2-negative control, and cytoplasmic ATF2 staining is shown in a breast cancer case for comparison.

(C) Immunofluorescence analysis of ATF2 nuclear localization in SYO-1 cells. Hoechst staining defines the nuclei.

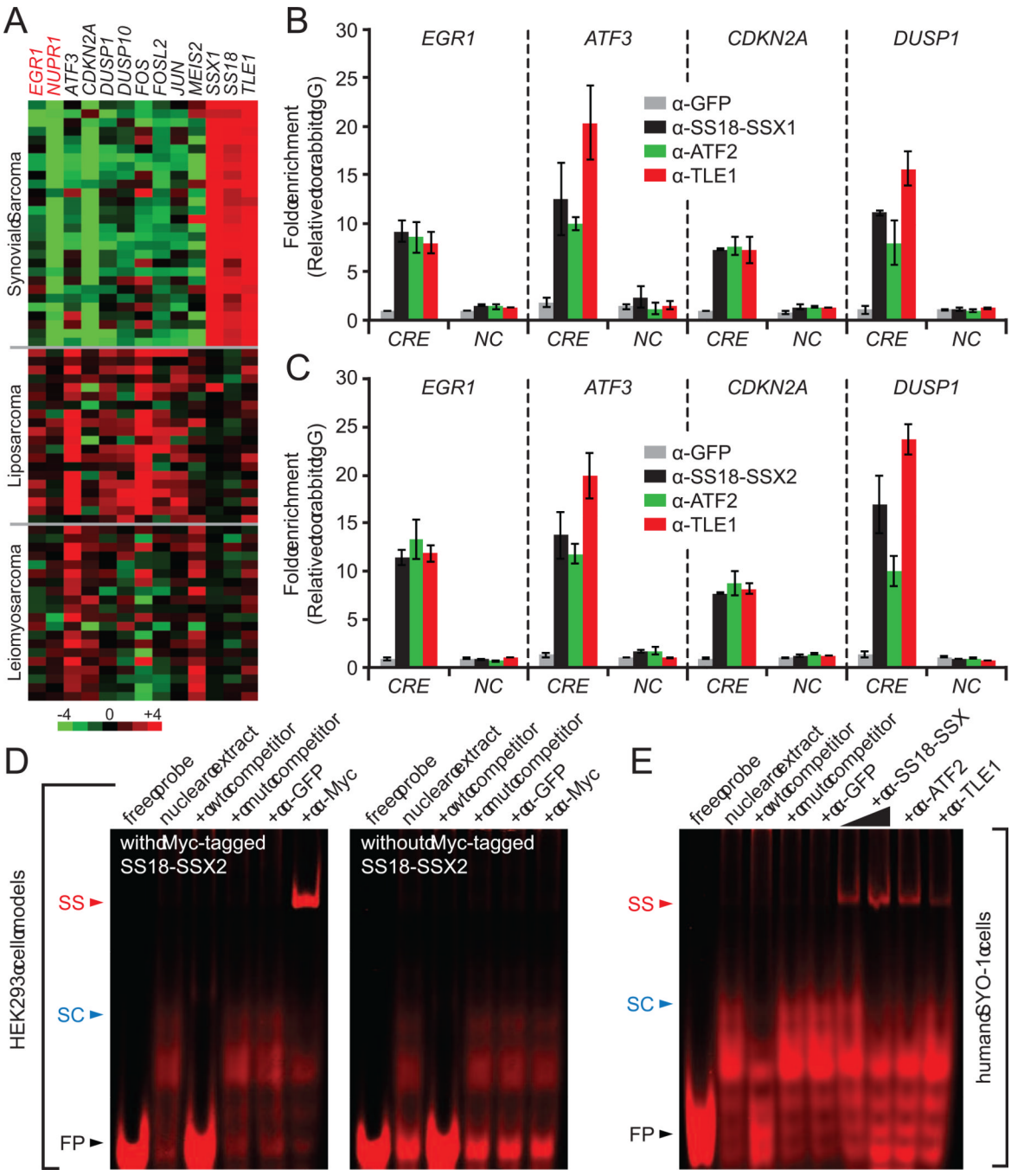

Figure 5. SS18-SSX is recruited to genes with an ATF/CRE element

(A) Heat map from meta-analysis of Affymetrix HG-U133_Plus_2 arrays, from Gene expression omnibus accessions GSE21050 (PMID 20581836) and GSE20196 (PMID: 20975339). Quantile normalized GCRMA expression values are given in log base 2, and calculated relative to the median expression for each gene. SS: synovial sarcoma; LPS liposarcoma; LMS: leiomyosarcoma.

(B and C) ChIP results of primary synovial sarcoma specimens showing SS18-SSX, ATF2, and TLE1 recruitment to the promoter regions of indicated genes. B and C, represent synovial sarcomas containing either SS18-SSX1 or SS18-SSX2 fusion oncoproteins, respectively. The ChIP enrichment was normalized to Rabbit IgG, anti-GFP ChIP was used

as the negative control and ChIP assays were also carried out using non-CRE (NC) containing portions of the respective gene promoters. Bar charts are mean +/− SD.
(D and E) Electrophoretic mobility shift assay competition and supershift assays showing SS18-SSX2 DNA-binding activity in HEK293 cell models (D) and SYO-1 cells (E). SS, supershift; SC, SS18-SSX:CRE complex; FP, free probe. See also Figure S4.

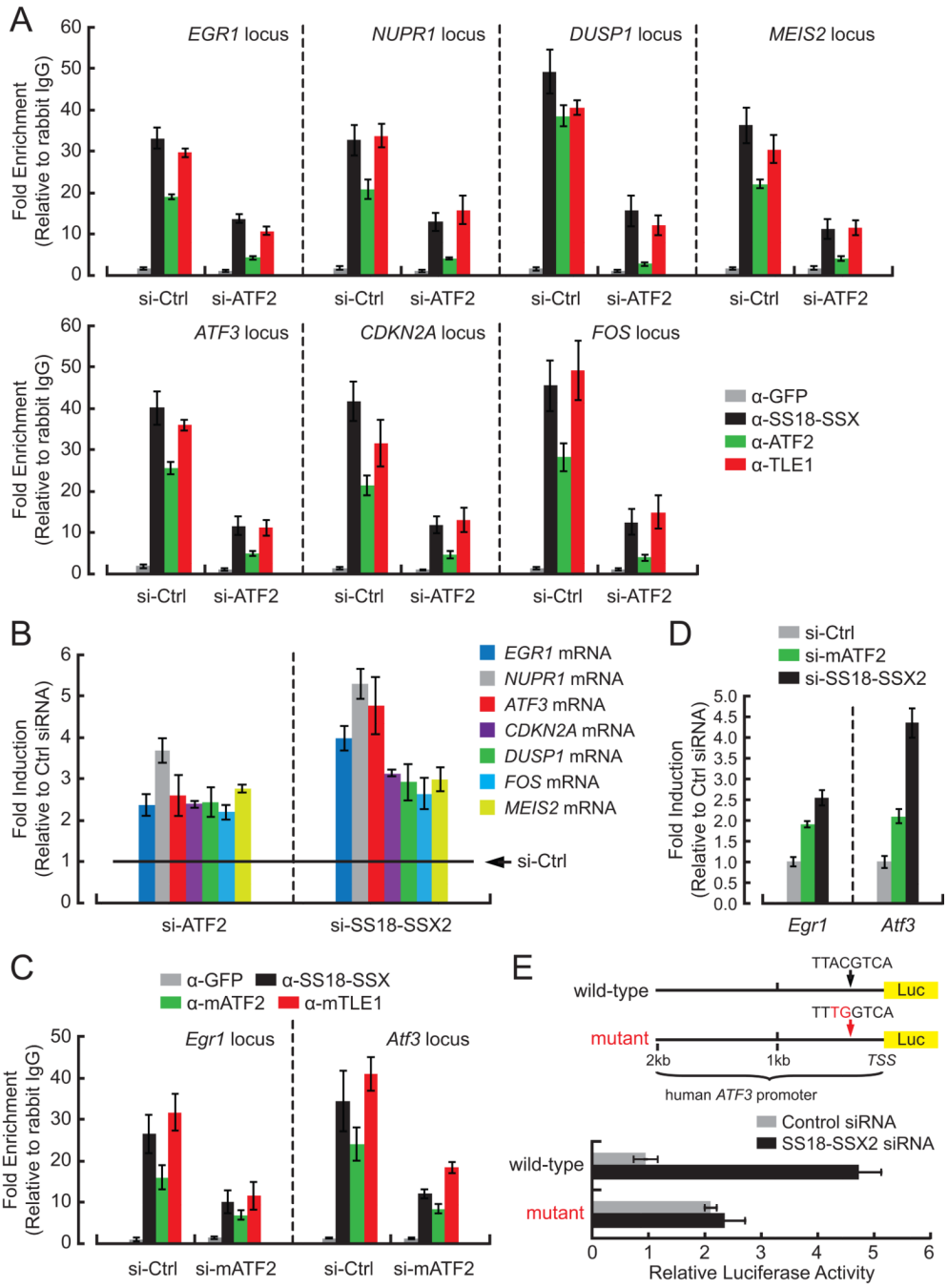

Figure 6. ATF2 is critical for DNA-binding of the SS18-SSX complex

(A and C) Binding of SS18-SSX, ATF2 and TLE1 to representative target promoters was determined by ChIP-qPCR in human SYO-1 (A) and mouse SS tumor cells (C) transfected with control or ATF2/mATF2 siRNA.

(B and D) RT-qPCR analysis of indicated ATF2 target gene expression in human SYO-1 cells (B) and mouse SS tumor cells (D) transfected with control, ATF2/mATF2, or SS18-SSX2 siRNA. Transcript levels were normalized to 18s rRNA, and depicted as a fold change between control and knockdown cells.

(E) Luciferase reporter assays showing the human *ATF3* promoter activity in control and SS18-SSX2 knockdown SYO-1 cells. The reporter constructs were made with the wild-type

ATF3 promoter regions with or without indicated base substitutions in the ATF/CRE site. All panels, bar charts are mean +/− SD. See also Figure S5.

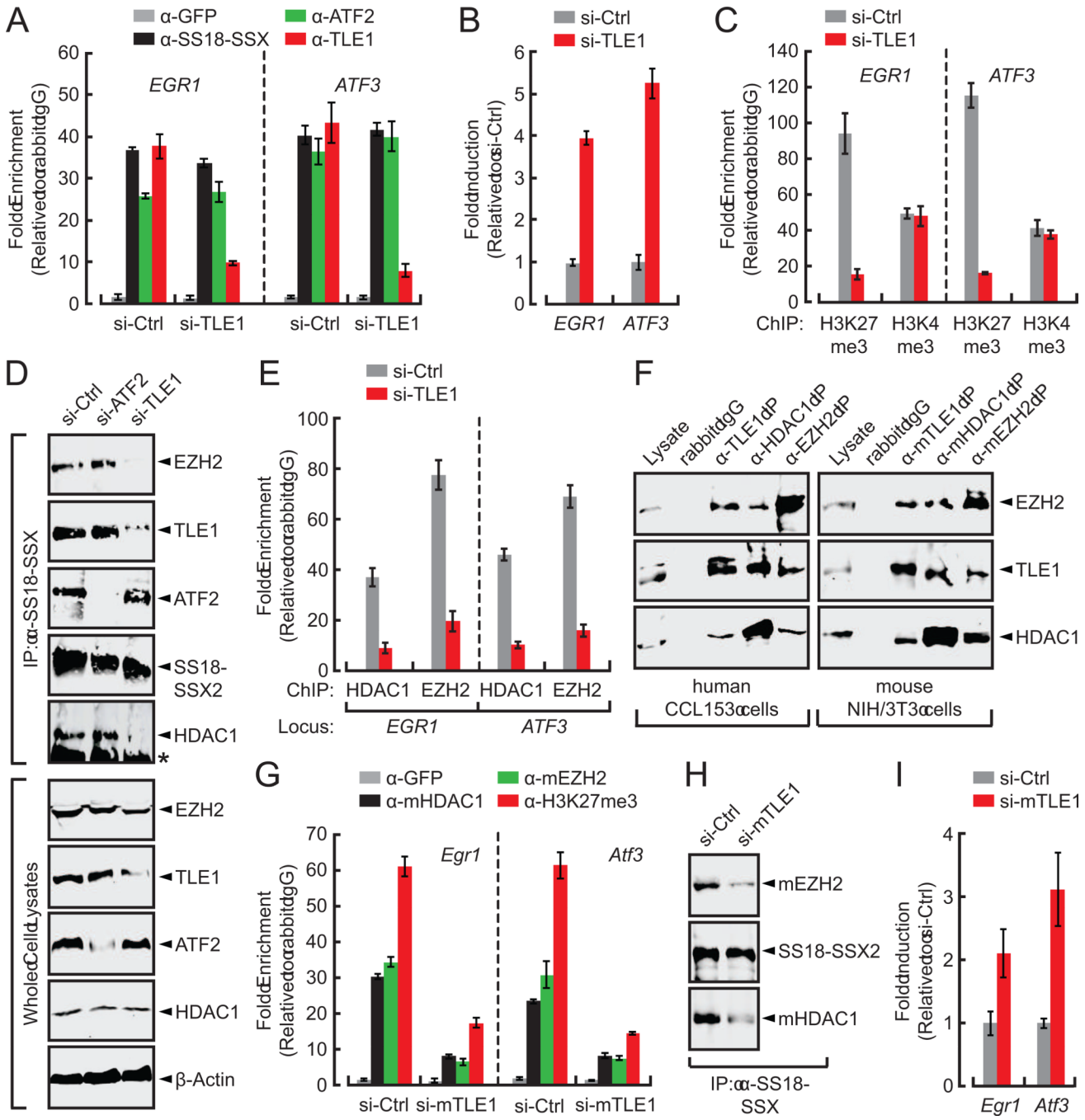

Figure 7. TLE1 contributes to SS18-SSX-mediated repression

(A, C, and E) ChIP-qPCR analysis of the human *EGR1* and *ATF3* promoters in control and TLE1 knockdown SYO-1 cells. The GFP antibody was used as a negative control for ChIP assays. Columns represent mean ± S.D. ($n = 3$).

(B) RT-qPCR analysis for human *EGR1* and *ATF3* gene transcripts in SYO-1 cells before and after TLE1 depletion. Transcript levels were normalized to 18s rRNA, and depicted as a fold change between control and TLE1 knockdown SYO-1 cells.

(D) SS18-SSX IP assay showing its association with HDAC1 and EZH2 in control, ATF2 and TLE1 knockdown SYO-1 cells. Asterisk indicates IgG bands.

(F) Reciprocal IP with the TLE1, HDAC1 and EZH2 antibodies showing their interaction in normal human (left) and mouse (right) fibroblast cells.
(G) ChIP-qPCR analysis of control and mTLE1 knockdown mouse synovial sarcoma cells using the indicated antibodies.
(H) Association of SS18-SSX2 with HDAC1 and EZH2 was determined by IP in mouse SS tumor cells transfected with control or mTLE1 siRNA.
(I) RT-qPCR analysis of *Egr1* and *Atf3* gene transcripts in mouse tumor cells transfected with control or mTLE1 siRNA for 48 hr. Changes in expression were normalized to control cells. Columns represent mean ±S.D. ($n = 3$). Bar charts are mean +/− SD. See also Figure S6.

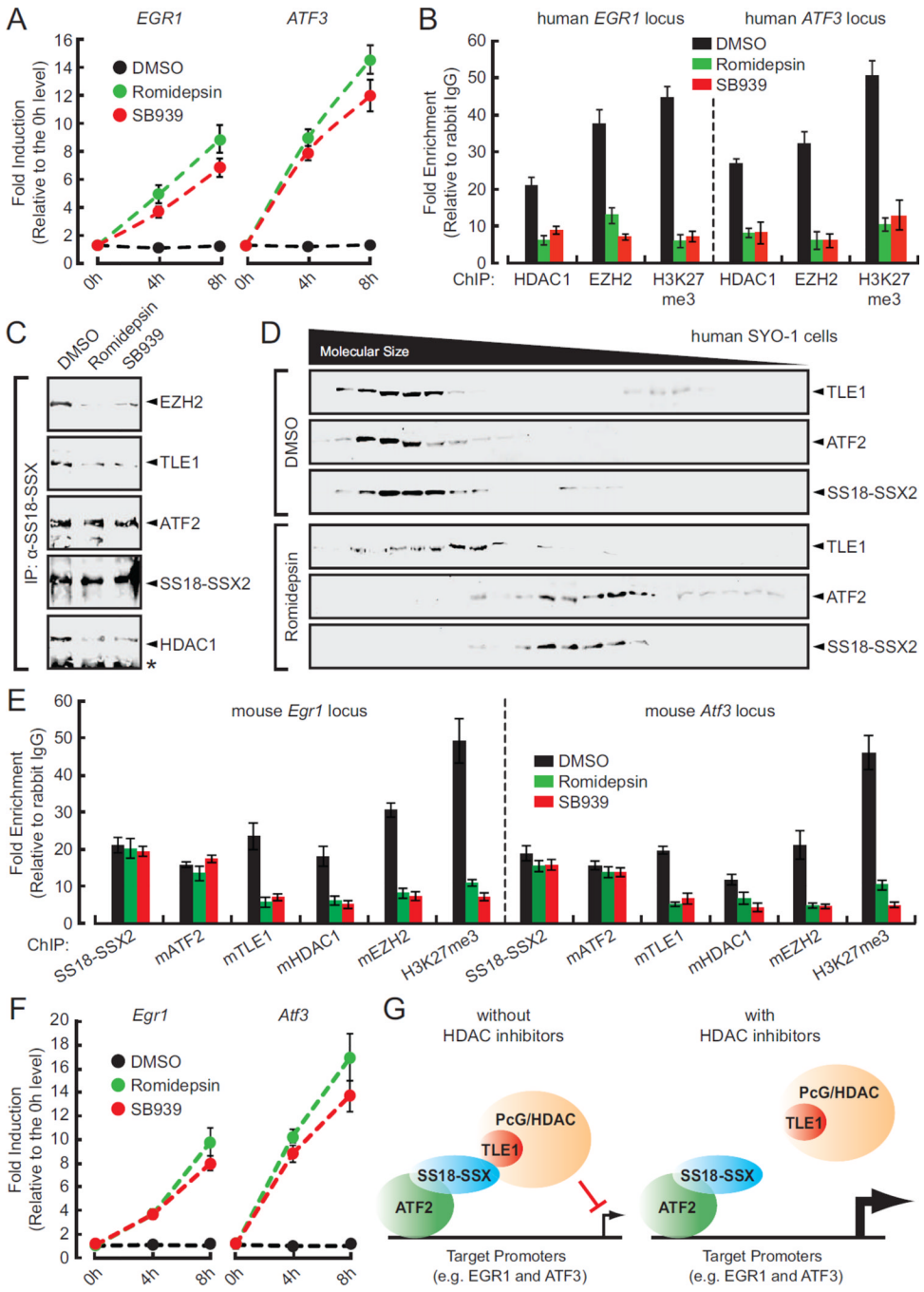

Figure 8. Effect of HDAC inhibitors on TLE1 recruitment and SS18-SSX-mediated gene silencing

(A) RT-qPCR analysis of human *EGR1* and *ATF3* gene transcripts in SYO-1 cells treated with DMSO, romidepsin, or SB939 for 8 hr. Changes in expression were normalized to the 0-hr time point.

(B and E) ChIP-qPCR analysis of the *EGR1* and *ATF3* promoters in SYO-1 and mouse synovial sarcoma cells treated with DMSO, romidepsin or SB939 for 8 hr. The antibodies used in ChIP assays are shown at the bottom of each panel.

(C) SS18-SSX IP assay in DMSO-, romidepsin- and SB939-treated SYO-1 cells. ATF2 and TLE1 protein levels were determined by western blot analysis of whole cell lysates (Fig. S7E). Asterisk indicates IgG bands.
(D) Glycerol-gradient sedimentation analysis of DMSO- and romidepsin-treated SYO-1 cell extracts 8h following treatment.
(F) Transcript levels for *Egr1* and *Atf3* were measured by RT-qPCR in mouse SS tumor cells treated with DMSO, romidepsin, or SB939 for 8 h, and depicted as a fold change relative to the 0-hr time point.
(G) Model of how the SS18-SSX complex regulates transcription before and after HDAC inhibitor treatment. Bar charts are mean +/− SD. See also Figure S7.